Intranasal delivery of deferoxamine reduces spatial memory loss in APP/PS1 mice

Leah R. Hanson, Jared M. Fine, Dan B. Renner, Aleta L. Svitak, Rachel B. Burns, Thuhien M. Nguyen, Nathan J. Tuttle, Dianne L. Marti, et al.

Drug Delivery and Translational Research
An Official Journal of the Controlled Release Society

ISSN 2190-393X

Drug Deliv. and Transl. Res.
DOI 10.1007/s13346-011-0050-2

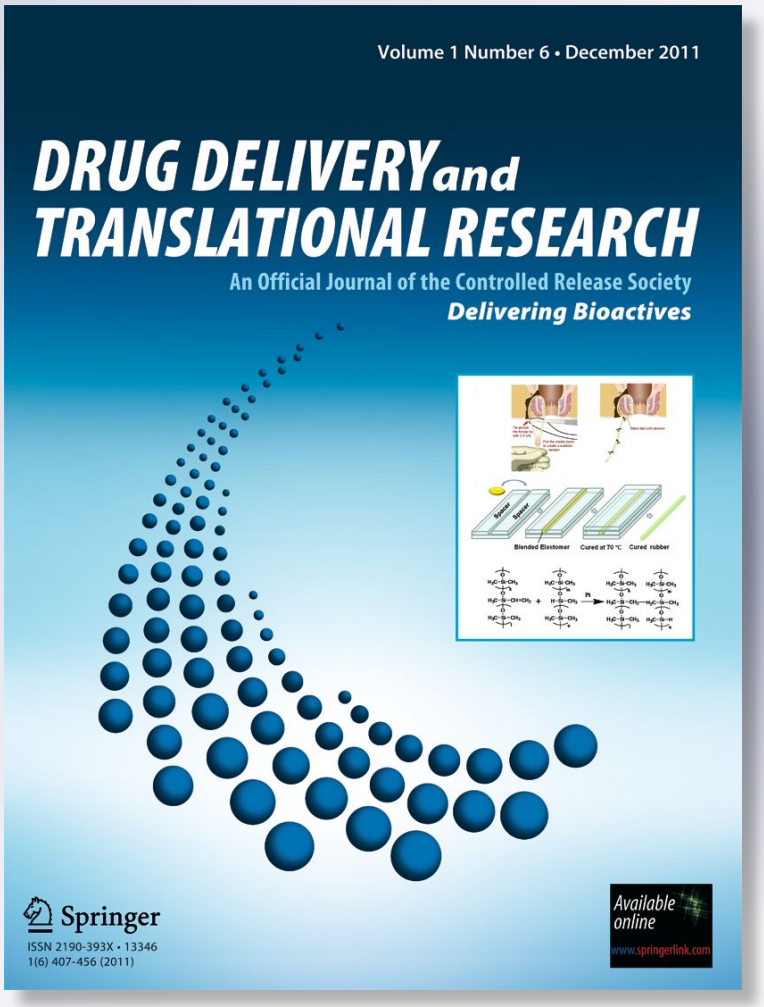

Springer

Drug Deliv. and Transl. Res.
DOI 10.1007/s13346-011-0050-2

RESEARCH ARTICLE

Intranasal delivery of deferoxamine reduces spatial memory loss in APP/PS1 mice

Leah R. Hanson · Jared M. Fine · Dan B. Renner · Aleta L. Svitak · Rachel B. Burns · Thuhien M. Nguyen · Nathan J. Tuttle · Dianne L. Marti · S. Scott Panter · William H. Frey II

Abstract Intranasal administration, which bypasses the blood–brain barrier and minimizes systemic exposure, is a non-invasive alternative for targeted drug delivery to the brain. While identification of metal dysregulation in Alzheimer's brain has led to the development of therapeutic metal-binding agents, targeting to the brain has remained an issue. The purpose of this study was to both determine concentrations of deferoxamine (DFO), a high-affinity iron chelator, reaching the brains of mice after intranasal administration and to determine its efficacy in a mouse model of spatial memory loss. Intranasal administration of DFO (2.4 mg) labeled with ^{59}Fe (75 μCi) to C57 mice resulted in micromolar concentrations at 30 min within brain parenchyma. After 3 months of intranasal DFO treatment, 2.4 mg three times per week, 48-week-old APP/PS1 mice had significantly reduced escape latencies in Morris water maze compared to vehicle-treated mice. This is the first report that intranasal DFO improves spatial memory in a mouse model of Alzheimer's disease and demonstrates that intranasal DFO reaches the brain in therapeutic doses.

L. R. Hanson (✉) · J. M. Fine · D. B. Renner · A. L. Svitak · R. B. Burns · T. M. Nguyen · N. J. Tuttle · D. L. Marti · W. H. Frey II
Alzheimer's Research Center at Regions Hospital, HealthPartners Research Foundation,
640 Jackson Street,
St. Paul, MN 55101, USA
e-mail: Leah.R.Hanson@HealthPartners.com

S. S. Panter
Department of Neurosurgery, San Francisco Veterans Affairs Medical Center and the University of California at San Francisco,
4150 Clement Avenue,
San Francisco, CA 94121, USA

Published online: 11 January 2012

Keywords Drug targeting · Alzheimer's disease · Morris water maze · Iron · Metals · Amyloid

Introduction

Intranasal (IN) delivery is a non-invasive method of targeting drugs to the central nervous system (CNS) along the olfactory and trigeminal nerve pathways from the nasal cavity. Benefits of IN delivery include minimizing systemic exposure and therefore side effects, and allowing large and/or charged molecules to bypass the blood–brain barrier to gain access to the CNS [1–4]. Direct delivery of a wide range of molecules to the CNS following IN administration has been demonstrated in rodents, primates, and humans [5–8]. In normal adults and in patients with amnestic mild cognitive impairment or in the early stages of AD, IN insulin has been shown to improve memory with no change in blood insulin or blood glucose [7, 9–11].

Chelators and other metal-binding agents are currently being developed as treatments for neurodegenerative disorders, such as Alzheimer's disease (AD) [12–14]. There are several ways by which chelators may be beneficial for AD. First, they can reduce the metal-catalyzed production of damaging reactive oxidative species (ROS) and/or increase the brain's ability to safely manage oxygen stress [12, 15]. Iron accumulates in the Alzheimer's brain, and overproduction of ROS or an inability to efficiently regulate ROS in the diseased state may result in the accumulation of tissue damage [16]. Alternatively, a different mechanism involving transient chelator exposure can induce the cell's stress response by activating neuroprotective signaling proteins such as hypoxia-inducible factor-1α (HIF-1α), NF-κB, and the iron response protein/iron response element.

Metal-binding agents developed for the treatment of AD include clioquinol, PBT2, and deferoxamine (DFO), which have been tested in clinical trials. Clioquinol was shown to cause a decrease in insoluble Aß in a transgenic mouse model [17]. In two clinical trials, it was concluded that clioquinol may have resulted in mild improvements in cognition and neuropathology [18, 19]; however, its efficacy has been questioned [20] and some toxic effects have been reported in transgenic mice [21]. More recently, a second generation 8-OH quinoline, PBT2, has undergone phase IIa clinical trials demonstrating it is well tolerated, alters putative CSF biomarkers for AD, and has cognitive efficacy in two measures of executive function [22]. Deferoxamine is an FDA approved chelator for iron overload disease. Intraperitoneal injections of DFO (three times per week for 2 weeks) to aged Wistar rats have been shown to reverse age-related memory impairment and reduce oxidative damage in cortex and hippocampus [23]. A clinical trial of intramuscular DFO (5 days per week) in AD patients demonstrated a 50% reduction in the rate of decline in daily living activities over 2 years [24, 25]. However, the use of DFO was not further pursued likely due to difficulty of delivery, rapid clearance, and limited blood–brain barrier permeability. In a rat model of ischemic stroke, intranasally administered DFO has been shown to target the CNS and reduce infarct volume by 55% without clinically significant changes in blood pressure or heart rate [26].

In this study, the distribution of a single dose of ^{59}Fe-labeled DFO was assessed 30 min after intranasal administration in C57 mice, and micromolar concentrations were observed in the CNS. The efficacy of IN DFO was assessed in a mouse model of AD and 3 months of treatment resulted in improved performance in the Morris Water maze test of spatial memory.

Materials and methods

Animal care and treatment

For radiolabeled pharmacokinetic studies, seven C57 male mice (age 6 weeks) were purchased from Harlan (Indianapolis, IN, USA). For behavior and subsequent biochemical tests, 24 male APP/PS1 transgenic mice and 12 wild-type controls were purchased from Jackson Laboratories (B6C3-Tg(APPswe,PSEN1dE9)85DBO/J; stock #004462; Bar Harbor, ME, USA). Mice arrived in our animal care facility (33 weeks old, mean weight 33.4 g) and were acclimated to handling for awake, IN delivery over a period of 3 weeks. Mice were kept on a regular light cycle and given standard rodent diet and water ad libitum.

For behavior and biochemical tests, mice were divided into three treatment groups and intranasally treated three times per week for 4 months as follows: (1) APP/PS1 mice treated with IN vehicle (24 μL, n=11); (2) APP/PS1 mice treated with IN DFO (2.4 mg in 24 μL, n=12); and (3) wild-type control mice treated with IN vehicle (24 μL, n=13). Sample sizes of 12 for all groups were originally planned, but one mouse identified as APP/PS1 that had been treated with IN vehicle did not show expression of humanized mutant APP as determined by western blot analysis, and was therefore moved into the wild-type control group for analysis. APP/PS1 mice were semi-randomly assigned to groups based on baseline performance in a Morris Water Maze before the start of treatment (hidden/visual platform and probe tests), as well as average weight and age. Deferoxamine mesylate salt was purchased from Sigma (D9533; St. Louis, MO, USA), and was administered as a 10% solution in 0.2× PBS (phosphate-buffered saline, Sigma P5493, diluted 1:5 in sterile water, diluted buffer) with a pH of 6.0. The vehicle consisted of 0.2×PBS without DFO. Mice were intranasally treated every Monday, Wednesday, and Friday for 4 months beginning at 36 weeks of age. For IN delivery, unanesthetized mice were gripped by the skin of their necks and held gently, but firmly upside-down in the palm of the hand. A 20-μl pipettor was used to administer four 6-μl nose drops (alternating nares; 24 μl total containing 2.4 mg DFO) to each mouse. The mouse was released for 2-min intervals between each pair of nasal drops [8].

^{59}Fe–DFO distribution with IN delivery

A mixture of DFO labeled with ^{59}Fe was delivered to seven C57 mice using the awake IN delivery method described above (24 μl total). The solution contained 10% DFO (2.4 mg) with 75 μCi of ^{59}Fe (Perkin Elmer; Waltham, MA, USA). It was prepared by mixing ^{59}Fe in 0.5 M HCl and the same amount of 0.5 M NaOH with 10% DFO in 25 mM sodium acetate buffer. There was a high molar ratio of DFO/^{59}Fe so all ^{59}Fe would be bound as ferrioxamine and most of the solution consisted of uncomplexed DFO. At 20 min after the onset of IN administration, mice were anesthetized with sodium pentobarbital. At 30 min after the onset of IN administration, blood was drawn from the heart, and mice were perfused with 20 mL saline followed by 120 mL 4% paraformaldehyde at a rate of 15 mL/min. Tissues were dissected, weighed, cut into 1×1×1 mm pieces, placed into scintillation fluid, and ^{59}Fe–DFO quantified with a scintillation counter (Beckman Coulter). Tissue solubilization for scintillation counting was not necessary because ^{59}Fe is a high-energy beta emitter. Concentrations of DFO were calculated based upon detected amounts of ^{59}Fe–DFO and the specific activity of known standards.

Morris water maze

Water maze tests were performed on APP/PS1 mice starting at 35 weeks of age prior to the start of IN administration (baseline tests), and after 3 months of IN DFO treatment. Treatment continued during behavior testing. The water maze was a round, flat-bottomed, black plastic tub (Polytank Inc., Litchfield, MN, USA) with a diameter at the surface of the water of 108 cm. Water was maintained at room temperature and non-toxic white paint was added to obstruct visibility, obscuring the hidden platform. Prominent visual cues surrounded the tank. Four drop points (1–4) were located starting at the observers left, and were distributed clockwise every quarter of the tank, respectively. The platform was a clear, plastic square of 9×9 cm placed 1 cm below the surface of the water for hidden platform tests. Tests with hidden platform were performed in eight successive blocks at two blocks per day (M–T–W–Th). Each block consisted of four trials of up to 60 s (with 20 s between trials to sit on the platform). Each trial was a drop at one of the four drop points and was always done in the same order (1, 2, 3, 4). Mice that did not reach the platform after 60 s were gently guided to the platform. The platform remained at the same location for baseline testing and the first four blocks of testing at 3 months. For the last four blocks, it was moved to a new location to make the test more challenging. Probe tests were conducted twice throughout the week, where the hidden platform was removed and mice were allowed to swim in the maze for 1 min. Probe 1 occurred Wednesday morning (before block 5), and probe 2 occurred Friday morning (after block 8). The percent time in each quadrant was measured. After the final probe, there was a visual platform test that was the same as the hidden platform test, except that the platform was black and remained visible just above the surface of the water. All water maze data was digitally acquired with an overhead camera connected to a DVD recorder. Data was analyzed using the EthoVision tracking system (Version 3.1; Noldus, Leesburg, VA, USA).

Escape latency, path length, and velocity were analyzed for hidden and visual platform tests. For probe tests, the percent time spent in the quadrant with the platform was analyzed. For hidden platform tests at baseline, the four trials were averaged for each block and the data analyzed with repeated measures analysis of variance (ANOVA) with Fisher's LSD post-test. Probe trials, visual platform trials, velocity, and hidden platform tests at 3 months were analyzed with ANOVA with Tukey's post-test. A significance level of $p<0.05$ was used.

Tissue collection

At 4 months after onset of IN DFO treatment, mice were anesthetized with sodium pentobarbital for euthanasia and tissue collection. Two mice died during the time between completion of the behavioral testing and tissue collection due to natural causes associated with aging, both in the APP/PS1 vehicle-treated group. Blood was drawn from the heart, and mice were perfused with 20 mL saline at a rate of 15 mL/min. The brain and body were dissected with metal-free instruments (approximately 20 tissue samples were collected per mouse) and snap-frozen in metal-free tubes with liquid nitrogen. These tissues were stored in a freezer at −80°C, which malfunctioned and the samples thawed, thereby preventing biochemical analyses. A portion of the left hemisphere including cortex and hippocampus were fixed in paraformaldehyde for IHC. The fixed tissue was stored at 4°C in a 30% sucrose solution. Tissue was then embedded in tragacanth gum, sectioned on a cryostat (10–20 μm) and stored at −80°C before further staining.

Metal analyses

Inductively coupled plasma mass spectroscopy (ICP-MS) was used to determine metal content in brain tissue. Frontal cortex, olfactory bulb, and midbrain tissue samples from each of the three experimental groups were pooled by tissue type and group to yield sample sizes ranging from 13 to 100 mg. Samples were run on an Agilent 7500ce (Foster City, CA, USA) and were analyzed for iron, aluminum, copper, and zinc. To prepare samples for ICP-MS, tissue was digested on a hot block with 1 mL of concentrated nitric acid and 0.5 mL of 30% hydrogen peroxide. The digest was diluted to a final mass of 5 g with nanopure water. A single pooled sample was analyzed for each tissue type.

Amyloid plaques

Plaque burden was quantified with immunohistochemistry using an Aβ-specific antibody (4G8; specific to amino acids 18–22). Coronal sections of hippocampus and cortex of DFO-treated ($n=12$) and vehicle-treated ($n=9$) groups of APP/PS1 mice and wild-type mice ($n=13$) were analyzed. Tissue sections were probed with a 1:1000 dilution of the monoclonal 4G8 antibody (Chemicon, cat# MAB1561) and secondary incubations included a 1:500 dilution of the rabbit anti-mouse HRP (Chemicon, cat# AP160P). Reactivity was visualized with enhanced DAB-peroxidase substrate solution (Pierce, cat # 34065). Six sections containing both hippocampus and cortex from each mouse were quantified by blinded investigators. A 6-megapixel image of each section was captured with an Olympus BH3 microscope and a Canon Powershot SD630 digital camera. Images were analyzed with Image J software (NIH) to identify total number and area of plaques. Additional particle analysis was conducted with three minimum pixel size limits to identify small (>25 μm), medium (25–50 μm), and large

plaques (>50 μm). *T* tests were used for comparison of plaques between IN DFO and vehicle-treated groups at each anatomical location.

Results

Biodistribution of IN DFO assessed with ^{59}Fe–DFO

The affinity of DFO for Fe is extremely high (10^{31}) allowing the use of ^{59}Fe–DFO as a stable radioactive tracer for assessing IN delivery of DFO to the brain. Within 30 min after IN administration (24 μL, 2.4 mg, 75 μCi), DFO was detected in all areas of the CNS. The highest concentrations of DFO within the CNS of C57 mice were observed along the olfactory and trigeminal pathways hypothesized to be involved with direct delivery of therapeutics from the nasal cavity to the CNS (olfactory bulb, 13 μM; trigeminal nerves, 29 μM; Table 1). The hypothalamus (4 μM) had the next highest DFO concentration. Concentrations ranging from 1.1 to 1.7 μM were also observed in structures proximal to the olfactory bulbs (anterior olfactory nucleus and frontal cortex) and to the trigeminal nerves (medulla and pons). Concentrations in other CNS structures ranged from 0.4 to 0.9 μM. High concentrations were also observed in the meninges (21 to 54 μM) and cervical lymph nodes (17 μM). Systemic exposure was highest in the kidney (8.5 μM), and a concentration of 5.2 μM was observed in the blood (Table 1).

Table 1 Tissue concentrations (micromolar) of deferoxamine (DFO) 30 min after intranasal administration to C57 mice of 3.65 μmol DFO (2.4 mg in 24 μL containing 75 μCi DFO–Fe^{59} tracer)

	Mean (μM) ± SEM[a]
Brain tissue	
Trigeminal nerve	29 ± 11
Olfactory bulbs	13 ± 6
Anterior olfactory nucleus	1.5 ± 0.4
Frontal cortex	1.7 ± 0.6
Striatum	0.6 ± 0.2
Hippocampus	0.8 ± 0.2
Thalamus	0.4 ± 0.1
Hypothalamus	4.1 ± 1.3
Midbrain	0.9 ± 0.3
Pons	1.4 ± 0.4
Medulla	1.1 ± 0.3
Cerebellum	0.7 ± 0.2
Spinal cord	
Cervical spinal cord	2.0 ± 0.7
Thoracic spinal cord	1.6 ± 0.4
Lumbar spinal cord	1.5 ± 0.4
Meninges	
Spinal meninges	21 ± 8
Ventral meninges	54 ± 16
Lymph nodes	
Superficial nodes	1.9 ± 0.5
Cervical nodes	17 ± 6
Axillary nodes	4.3 ± 1.6
Peripheral tissues	
Blood at 30 min	5.2 ± 1.5
Liver	0.7 ± 0.2
Kidney	8.5 ± 2.2
Muscle	0.8 ± 0.1
Heart	0.7 ± 0.1
Lung	1.0 ± 0.2

[a] Sample size of 5–7

IN DFO improved Morris water maze performance in APP/PS1 mice

Intranasal treatment of APP/PS1 mice with DFO decreased escape latencies and path length in Morris water maze hidden platform tests. Mice were divided into three treatment groups and intranasally treated three times per week in the following groups: (1) APP/PS1 mice treated with IN vehicle (n=11); (2) APP/PS1 mice treated with IN DFO (2.4 mg/dose, n=12); and (3) wild-type control mice treated with IN vehicle (n=13). No significant differences in escape latencies or path length between the three groups were identified at baseline prior to initiation of treatment (Fig. 1a, b). After 3 months of treatment, IN DFO-treated APP/PS1 mice had significantly shorter escape latencies and path length compared to vehicle-treated APP/PS1 mice by block 4 of hidden platform testing (p<0.01, Fig. 1c, d). In addition, the performance of DFO-treated APP/PS1 mice at block 4 was not statistically different than vehicle-treated wild-type mice. When the platform was moved after block 4 to increase the challenge of the test, DFO-treated APP/PS1 mice, again, had improved performance versus vehicle-treated APP/PS1 mice as measured by significantly decreased escape latency in blocks 7 and 8.

In the first probe trial, wild-type control mice spent significantly more time in the quadrant that used to contain the platform than transgenic mice, but there was no difference between DFO and vehicle-treated APP/PS1 groups (data not shown, p<0.01). There were no significant differences in the second probe trial. In visual trials, there was no difference between DFO and vehicle-treated transgenic mice (data not shown). All mice were unimpaired and could easily complete water maze trials, but wild-type mice did have significantly shorter escape latencies than both groups of transgenic mice (p<0.05). During the hidden platform tests, there were no differences in velocity, but there was a

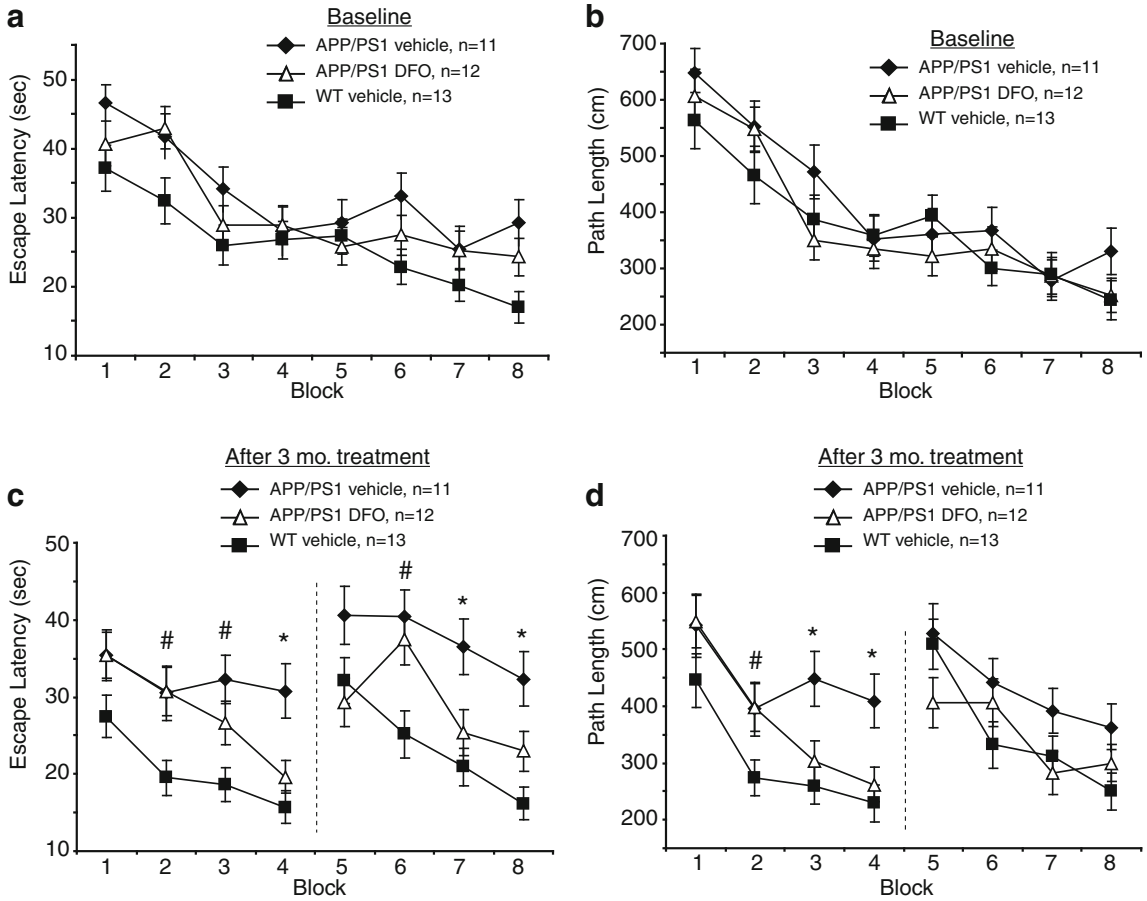

Fig. 1 Escape latency and path length for hidden platform Morris water maze tests in wild-type (WT) and APP/PS1 mice starting at baseline (35 weeks of age) and after 3 months of intranasal (IN) treatment three times per week with 24 μL containing either 2.4 mg deferoxamine (DFO) or vehicle. Values are means±standard error. During the 3-month testing, the hidden platform was moved after block 4 to make the test more challenging (indicated by the *dashed line*). **a** At baseline, no significant differences in escape latency were observed between WT and APP/PS1 mice or between the vehicle and DFO-treated groups of APP/PS1 mice (repeated measures ANOVA). **b** Similarly, there were no significant differences in path length between groups at baseline. **c** After 3 months of IN treatment, at blocks 4, 7, and 8, both WT mice and APP/PS1 mice treated with DFO had shorter escape latencies than vehicle-treated APP/PS1 mice (*$p<0.05$). At blocks 2, 3, and 6, WT mice had shorter escape latencies than both APP/PS1 groups (#$p<0.05$). **d** APP/PS1 mice treated with DFO and vehicle-treated WT mice had significantly shorter path lengths than vehicle-treated APP/PS1 mice at blocks 3 and 4 (*$p<0.05$). At block 2, WT mice had significantly shorter path lengths than both APP/PS1 groups (#$p<0.05$)

trend for wild-type mice to swim faster than both groups of APP/PS1 mice (data not shown).

Tolerability of 4 months IN DFO treatment of APP/PS1 mice

Intranasal DFO (2.4 mg in 24 μL of diluted buffer) was well tolerated as administered three times per week (Monday, Wednesday, Friday) over 4 months. There were no deaths or obvious physical side effects in the DFO-treated group. Only two mice died during the course of the study, both of which were APP/PS1 mice in the vehicle only group and deaths were due to natural causes related to aging. At the end of the 4-month administration period, no significant differences in body weight between treatment groups were observed (ANOVA, average weights±SE, DFO-treated APP/PS1 34±2 g, vehicle-treated APP/PS1 37±3 g, and vehicle-treated wild-type 35±1 g).

IN DFO reduced brain levels of aluminum

The only metal in the brain to show consistent changes with IN DFO treatment across the different brain regions tested was aluminum (Fig. 2). Intranasal DFO decreased aluminum concentrations in pooled samples of olfactory bulb, frontal cortex, and midbrain to 57%, 27%, and 39%, respectively, compared to those found in pooled samples of vehicle-treated APP/PS1 mice. Levels of total brain iron, zinc, and copper in the brain were relatively unaffected by IN DFO treatment.

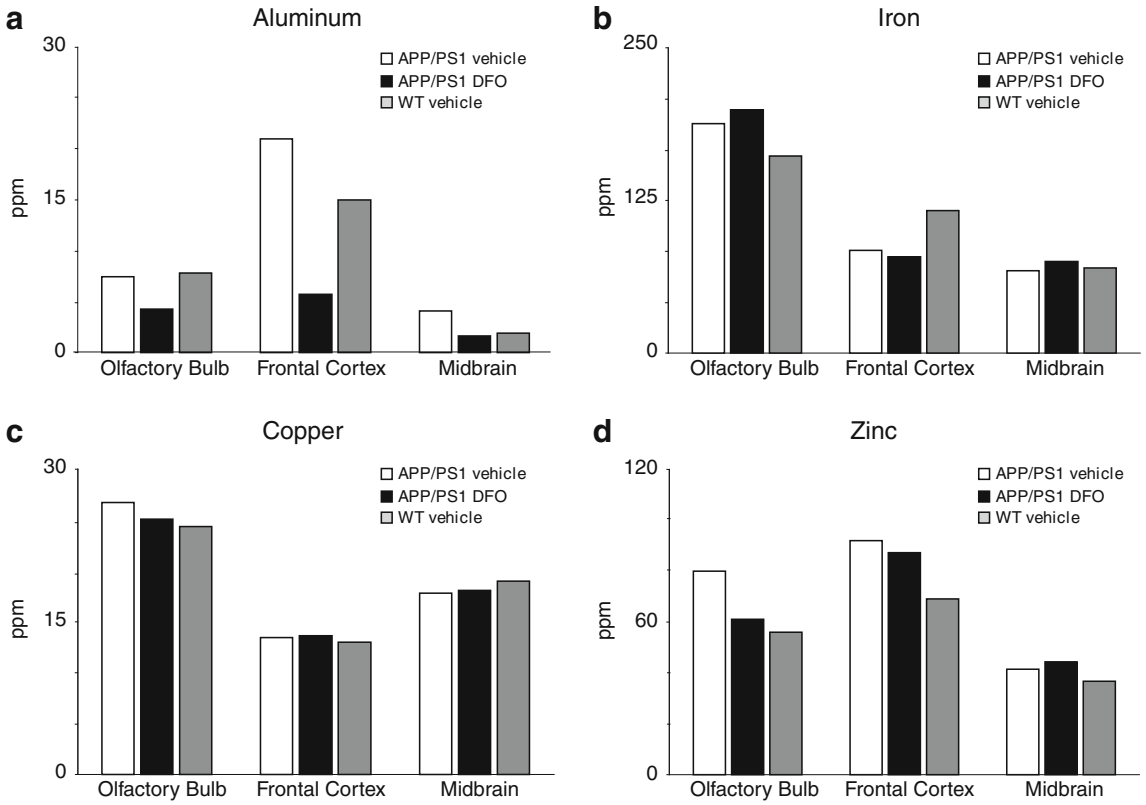

Fig. 2 Quantification of total brain levels of metals in pooled samples of wild-type (WT) and APP/PS1 mice after 4 months of intranasal (IN) treatment three times per week with 24 μL containing either 2.4 mg DFO or vehicle deferoxamine (DFO). Inductively coupled plasma mass spectrometry was performed on pooled samples of olfactory bulb, frontal cortex, or midbrain tissue from each group. Metal testing included: **a** aluminum, **b** iron, **c** copper, **d** zinc. The only consistent change in metal levels across different brain regions was the reduction in aluminum in APP/PS1 DFO-treated mice

IN DFO did not alter amyloid plaque deposition

Plaques were evident in both DFO and vehicle-treated APP/PS1 mice, while absent from wild-type mice. Intranasal DFO treatment did not significantly alter the total plaque number or total plaque area in the cortex or hippocampus of APP/PS1 mice (Fig. 3). To further explore a possible amyloid modulating effect, additional analysis of plaque deposition by size was

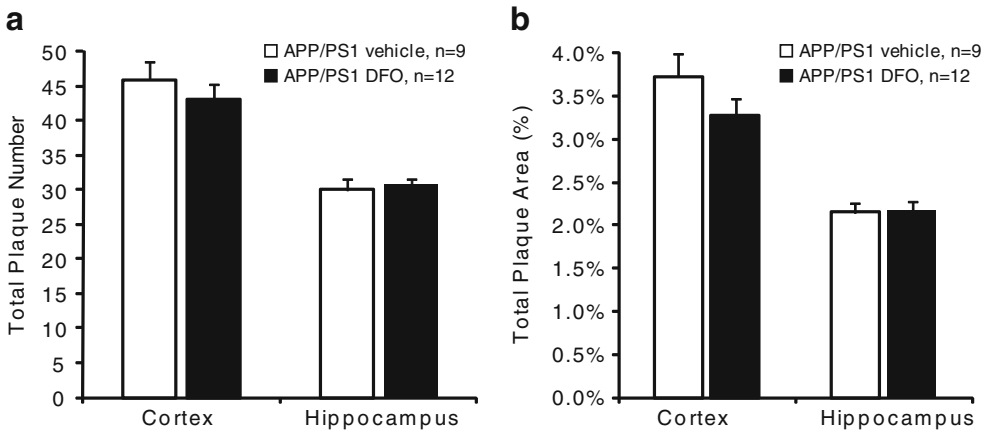

Fig. 3 Immunohistochemical measurement of amyloid plaques within the cortex and hippocampus of deferoxamine (DFO) and vehicle-treated APP/PS1 mice at 52 weeks of age. Starting at 36 weeks of age, mice were treated intranasally (IN) for 4 months, three times per week with 24 μL containing either 2.4 mg DFO or vehicle. No plaques were observed in wild type (WT) mice. Values are means±standard error. **a** No significant difference in the total plaque number was found between vehicle and DFO-treated APP/PS1 mice in either the cortex or hippocampus. **b** Similarly, there were no significant changes in total plaque area

conducted (% area and number of plaques less than 25, 25–50, and greater than 50 μm), but revealed no significant effect of IN DFO on amyloid plaque with the exception of a small (24%) decrease in the total area of plaques greater than 50 μm in the cortex (data not shown).

Discussion

These results demonstrate that IN DFO reaches the CNS in therapeutic doses and can reduce memory loss in a mouse model of amyloid accumulation. Significant improvement in performance of IN DFO-treated APP/PS1 mice in the Morris water maze, a measure of spatial memory function, was observed after 3 months of treatment. Micromolar concentrations of DFO were measured in the CNS of C57 mice 30 min after a single intranasal dose. Reduction of aluminum in the CNS after chronic IN DFO treatment of APP/PS1 mice provides further evidence that DFO achieved significant concentrations in the CNS, as DFO chelates aluminum and is used off-label for aluminum toxicity [27]. Brain concentrations of total iron, copper, and zinc in pooled samples were unaffected. The stability constants of DFO for Fe(III) and Al(III) (10^{31} and 10^{25}) are much stronger than Cu(II) and Zn(II) (10^{14} and 10^{11}) [28]. With micromolar brain concentrations and the strong affinity of DFO for free iron, IN DFO would undoubtedly chelate and reduce concentrations of free iron in the brain. However, this would not necessary be reflected in measurements of total brain iron, since free iron is a small portion of total brain iron. Decreasing free iron with DFO has been shown to induce downstream neuroprotective signaling pathways [29], which may have contributed to improved memory function observed in this study.

The distribution profile of DFO 30 min after IN administration in C57 mice is consistent with previously published results for IN DFO in rats [26]. In both studies, particularly high concentrations of DFO were detected in the olfactory bulbs, trigeminal nerve, hypothalamus, and the dura mater. This distribution is consistent with those of other intranasally administered compounds we and others have studied and with the hypothesis that IN delivery to the brain involves extracellular transport along the perineuronal space surrounding the olfactory nerve bundles, along the trigeminal nerves, and through the perivascular spaces surrounding the blood vessels [30–32]. It has been previously demonstrated that intranasal administration increased targeting of DFO to the brain as compared to intravenous delivery [26]. Targeting ratios (brain concentration/blood concentration after IN divided by the same ratio after intravenous) of about 200 across the brain indicated more targeted delivery with intranasal administration. Intranasal delivery is not receptor-mediated, and IN administration has been shown to deliver many small molecules of differing size and charge to the brain with roughly similar efficiency and brain distribution. One of the limitations of this study is that the ^{59}Fe–DFO complex was used as an indirect measure of DFO concentration and it may have different pharmacokinetic properties after intranasal administration. However, previous studies of intranasally administered compounds have shown similar concentrations and distribution of radiolabeled compared to non-labeled proteins using ELISA detection ([33], Hanson et al. unpublished). This experiment in C57 mice was an important proof of concept step that demonstrated micromolar concentrations of DFO reached the CNS, and was conducted prior to initiating lengthy and costly testing in the AD mouse model. Future studies will need to address the pharmacokinetics of IN DFO to understand its bioavailability and clearance in chronic dosing regimens.

DFO treatment of APP/PS1 mice resulted in significantly shorter escape latencies and path length than vehicle-treated mice in hidden platform trials using the Morris water maze. Visual platform tests and velocity data demonstrated that differences in spatial memory performance were not likely explained by changes in vision or speed. A limitation of this study is that it did not include an IN-DFO treated wild-type group. Future studies examining IN DFO effects in wild-type and other Alzheimer's mouse models are planned. While it has been reported that memory deficits in this APP/PS1 mouse model of amyloid accumulation are observed by 6 months of age [34], our baseline trials at 8 months of age did not detect a deficit in the transgenic mice. It is possible that the daily handling during acclimation necessary for IN administration to unanesthetized mice provided a type of environmental enrichment, which has been shown to mask memory impairment in behavioral testing of AD transgenic mice [35–37].

The mechanism by which IN DFO led to improved memory performance in this study remains unclear, though these results demonstrate it is not related to reduction of amyloid plaque burden. This was unexpected as metal ions, including Al, Fe, Cu, and Zn can facilitate the formation of plaques and DFO has been shown to block Fe- and Al-induced aggregation of amyloid β [38]. It is known that immunohistochemical assessment of plaques is not sufficient to understand the relationship between amyloid burden and performance in Morris water maze [39]. Future studies are planned to include analysis of soluble amyloid β protein levels. However, there are other amyloid-independent mechanism by which DFO may be neuroprotective. DFO eliminates excess, loosely bound, redox-active iron that could otherwise generate damaging levels of ROS [40, 41]. In animal models of stroke, DFO can induce neuroprotection by sequestering the LIP (labile iron pool), resulting in the activation of the HIF-1α response [42–44]. This response triggers gene expression shifts that increase the ability of the cell to deal with elevated levels of oxidative stress. Neuroprotection induced by the

HIF-1α response could reasonably account for the observed improvement in memory performance and is more likely than a general reduction in oxidative stress as the dosing regimen was three times per week as opposed to daily. Additional LIP-sensitive responses, such as the iron-response protein/iron-response element and NF-κB signaling may also be involved. Future studies are planned to identify the most significant mechanism(s) contributing to the observed behavioral improvement.

Conclusions

Intranasal DFO shows promise for the treatment of AD. Intramuscular injections of DFO have been shown to significantly delay loss of function in one trial with AD patients [24]. Intranasal delivery targets DFO to the CNS and offers a non-invasive alternative to injections or infusions, which can be associated with side effects. In one reported study in which DFO was delivered intranasally to humans for the purpose of treating iron-overload, side effects were few and consisted mainly of nasal irritation and bad taste in the mouth [45]. This is the first report in which DFO has been shown to improve the memory deficit in a transgenic mouse model of AD. Intranasally administered DFO did not appear to induce obvious side effects, and vision and weight in mice were unaffected. In summary, these results demonstrate that IN DFO reaches the CNS in therapeutic doses and can reduce memory loss in an AD mouse model, suggesting that IN DFO is an effective, non-invasive alternative for therapeutic delivery of DFO to the CNS.

Acknowledgments Thanks to Julian Tokarev and Kate Faltesek for their help with the behavior tests. Thanks to Thomas Flottemesch for assistance with the statistical analyses. Funding for this work was received from the HealthPartners Research Foundation Internal Grant 05-097 and private donations made to the Alzheimer's Research Center at Regions Hospital.

Ethical standards All experimental procedures were in compliance with the Guide for the Care and Use of Laboratory Animals and approved by the AAALAC accredited Health Partners Research Foundation's Animal Care and Use Program.

Declaration of interest LRH, SSP, and WHF are inventors on patents owned by the HealthPartners Research Foundation related to intranasal deferoxamine. All authors, except SSP, were employed by the HealthPartners Research Foundation during the time this work was conducted.

References

1. Vyas TK, Shahiwala A, Marathe S, Misra A. Intranasal drug delivery for brain targeting. Curr Drug Deliv. 2005;2:165–75.
2. Costantino HR, Illum L, Brandt G, Johnson PH, Quay SC. Intranasal delivery: physicochemical and therapeutic aspects. Int J Pharm. 2007;337:1–24.
3. Nonaka N, Farr SA, Kageyama H, Shioda S, Banks WA. Delivery of galanin-like peptide to the brain: targeting with intranasal delivery and cyclodextrins. J Pharmacol Exp Ther. 2008;325:513–9.
4. Dhanda DS, Frey WHI, Leopold D, Kompella UB. Approaches for drug deposition in the human olfactory epithelium. Drug Deliv. 2005;5:64–72.
5. Charlton ST, Whetstone J, Fayinka ST, Read KD, Illum L, Davis SS. Evaluation of direct transport pathways of glycine receptor antagonists and an angiotensin antagonist from the nasal cavity to the central nervous system in the rat model. Pharm Res. 2008;25:1531–43.
6. Thorne RG, Hanson LR, Ross TM, Tung D, Frey 2nd WH. Delivery of interferon-beta to the monkey nervous system following intranasal administration. Neuroscience. 2008;152:785–97.
7. Benedict C, Hallschmid M, Schultes B, Born J, Kern W. Intranasal insulin to improve memory function in humans. Neuroendocrinology. 2007;86:136–42.
8. Hanson LR, Martinez PM, Taheri S, Kamsheh L, Mignot E, Frey WHI. Intranasal administration of hypocretin 1 (Orexin A) bypasses the blood–brain barrier & targets the brain: a new strategy for the treatment of narcolepsy. Drug Deliv Tech. 2004;4:81–6.
9. Benedict C, Hallschmid M, Hatke A, Schultes B, Fehm HL, Born J, et al. Intranasal insulin improves memory in humans. Psychoneuroendocrinology. 2004;29:1326–34.
10. Reger MA, Watson GS, Frey 2nd WH, Baker LD, Cholerton B, Keeling ML, et al. Effects of intranasal insulin on cognition in memory-impaired older adults: modulation by APOE genotype. Neurobiol Aging. 2006;27:451–8.
11. Craft S, Baker LD, Montine TJ, Minoshima S, Watson GS, Claxton A, et al. Intranasal insulin therapy for alzheimer disease and amnestic mild cognitive impairment: a pilot clinical trial. Arch Neurol. 2011; (in press)
12. Domingo JL. Aluminum and other metals in Alzheimer's disease: a review of potential therapy with chelating agents. J Alzheimers Dis. 2006;10:331–41.
13. Crouch PJ, White AR, Bush AI. The modulation of metal bioavailability as a therapeutic strategy for the treatment of Alzheimer's disease. FEBS J. 2007;274:3775–83.
14. Bush AI. Drug development based on the metals hypothesis of Alzheimer's disease. J Alzheimers Dis. 2008;15:223–40.
15. Almli LM, Hamrick SE, Koshy AA, Tauber MG, Ferriero DM. Multiple pathways of neuroprotection against oxidative stress and excitotoxic injury in immature primary hippocampal neurons. Brain Research Dev Brain Res. 2001;132:121–9.
16. Altamura S, Muckenthaler MU. Iron toxicity in diseases of aging: Alzheimer's disease, Parkinson's disease and atherosclerosis. J Alzheimers Dis. 2009;16:879–95.
17. Cherny RA, Atwood CS, Xilinas ME, Gray DN, Jones WD, McLean CA, et al. Treatment with a copper-zinc chelator markedly and rapidly inhibits beta-amyloid accumulation in Alzheimer's disease transgenic mice. Neuron. 2001;30:665–76.
18. Regland B, Lehmann W, Abedini I, Blennow K, Jonsson M, Karlsson I, et al. Treatment of Alzheimer's disease with clioquinol. Dement Geriatr Cogn Disord. 2001;12:408–14.
19. Ritchie CW, Bush AI, Mackinnon A, Macfarlane S, Mastwyk M, MacGregor L, et al. Metal-protein attenuation with iodochlorhydroxyquin (clioquinol) targeting Abeta amyloid deposition and toxicity in Alzheimer disease: a pilot phase 2 clinical trial. Arch Neurol. 2003;60:1685–91.
20. Sampson E, Jenagaratnam L, McShane R. Metal protein attenuating compounds for the treatment of alzheimer's disease. Cochrane Database Syst Rev. 2008;CD005380.

21. Schafer S, Pajonk FG, Multhaup G, Bayer TA. Copper and clioquinol treatment in young APP transgenic and wild-type mice: effects on life expectancy, body weight, and metal-ion levels. J Mol Med. 2007;85:405–13.
22. Lannfelt L, Blennow K, Zetterberg H, Batsman S, Ames D, Harrison J, et al. Safety, efficacy, and biomarker findings of PBT2 in targeting Abeta as a modifying therapy for Alzheimer's disease: a phase IIa, double-blind, randomised, placebo-controlled trial. Lancet Neurol. 2008;7:779–86.
23. de Lima MN, Dias CP, Torres JP, Dornelles A, Garcia VA, Scalco FS, et al. Reversion of age-related recognition memory impairment by iron chelation in rats. Neurobiol Aging. 2008;29:1052–9.
24. Crapper McLachlan DR, Dalton AJ, Kruck TP, Bell MY, Smith WL, Kalow W, et al. Intramuscular desferrioxamine in patients with Alzheimer's disease. Lancet. 1991;337:1304–8.
25. McLachlan DR, Fraser PE, Dalton AJ. Aluminium and the pathogenesis of Alzheimer's disease: a summary of evidence. CIBA Found Symp. 1992;169:87–98. discussion 99–108.
26. Hanson LR, Roeytenberg A, Martinez PM, Coppes VG, Sweet DC, Rao RJ, et al. Intranasal deferoxamine provides increased brain exposure and significant protection in rat ischemic stroke. J Pharmacol Exp Ther. 2009;330:679–86.
27. Kan WC, Chien CC, Wu CC, Su SB, Hwang JC, Wang HY. Comparison of low-dose deferoxamine versus standard-dose deferoxamine for treatment of aluminium overload among haemodialysis patients. Nephrol Dial Transplant. 2010;25:1604–8.
28. Halliwell B. Protection against tissue damage in vivo by desferrioxamine: what is its mechanism of action? Free Radic Biol Med. 1989;7:645–51.
29. Wu Y, Li X, Xie W, Jankovic J, Le W, Pan T. Neuroprotection of deferoxamine on rotenone-induced injury via accumulation of HIF-1alpha and induction of autophagy in SH-SY5Y cells. Neurochem Int. 2010;57:198–205.
30. Hadaczek P, Yamashita Y, Mirek H, Tamas L, Bohn MC, Noble C, et al. The "perivascular pump" driven by arterial pulsation is a powerful mechanism for the distribution of therapeutic molecules within the brain. Mol Ther. 2006;14:69–78.
31. Thorne RG, Frey 2nd WH. Delivery of neurotrophic factors to the central nervous system: pharmacokinetic considerations. Clin Pharmacokinet. 2001;40:907–46.
32. Dhuria SV, Hanson LR, Frey 2nd WH. Intranasal delivery to the central nervous system: mechanisms and experimental considerations. J Pharm Sci. 2010;99:1654–73.
33. Chen XQ, Fawcett JR, Rahman YE, Ala TA, Frey IW. Delivery of nerve growth factor to the brain via the olfactory pathway. J Alzheimers Dis. 1998;1:35–44.
34. Trinchese F, Liu S, Battaglia F, Walter S, Mathews PM, Arancio O. Progressive age-related development of Alzheimer-like pathology in APP/PS1 mice. Ann Neurol. 2004;55:801–14.
35. Berardi N, Braschi C, Capsoni S, Cattaneo A, Maffei L. Environmental enrichment delays the onset of memory deficits and reduces neuropathological hallmarks in a mouse model of Alzheimer-like neurodegeneration. J Alzheimers Dis. 2007;11:359–70.
36. Costa DA, Cracchiolo JR, Bachstetter AD, Hughes TF, Bales KR, Paul SM, et al. Enrichment improves cognition in AD mice by amyloid-related and unrelated mechanisms. Neurobiol Aging. 2007;28:831–44.
37. Jankowsky JL, Melnikova T, Fadale DJ, Xu GM, Slunt HH, Gonzales V, et al. Environmental enrichment mitigates cognitive deficits in a mouse model of Alzheimer's disease. J Neurosci. 2005;25:5217–24.
38. House E, Collingwood J, Khan A, Korchazkina O, Berthon G, Exley C. Aluminium, iron, zinc and copper influence the in vitro formation of amyloid fibrils of Abeta42 in a manner which may have consequences for metal chelation therapy in Alzheimer's disease. J Alzheimers Dis. 2004;6:291–301.
39. Westerman MA, Cooper-Blacketer D, Mariash A, Kotilinek L, Kawarabayashi T, Younkin LH, et al. The relationship between Abeta and memory in the Tg2576 mouse model of Alzheimer's disease. J Neurosci. 2002;22:1858–67.
40. Hershko C, Weatherall DJ. Iron-chelating therapy. Crit Rev Clin Lab Sci. 1988;26:303–45.
41. Kontoghiorghes GJ. Comparative efficacy and toxicity of desferrioxamine, deferiprone and other iron and aluminium chelating drugs. Toxicol Lett. 1995;80:1–18.
42. Mu D, Chang YS, Vexler ZS, Ferriero DM. Hypoxia-inducible factor 1alpha and erythropoietin upregulation with deferoxamine salvage after neonatal stroke. Exp Neurol. 2005;195:407–15.
43. Freret T, Valable S, Chazalviel L, Saulnier R, Mackenzie ET, Petit E, et al. Delayed administration of deferoxamine reduces brain damage and promotes functional recovery after transient focal cerebral ischemia in the rat. Eur J Neurosci. 2006;23:1757–65.
44. Prass K, Ruscher K, Karsch M, Isaev N, Megow D, Priller J, et al. Desferrioxamine induces delayed tolerance against cerebral ischemia in vivo and in vitro. J Cereb Blood Flow Metab. 2002;22:520–5.
45. Gordon GS, Ambruso DR, Robinson WA, Githens JH. Intranasal administration of deferoxamine to iron overloaded patients. Am J Med Sci. 1989;297:280–4.